Effective Synthesis of Patterned Polymer Brushes with Tailored Multiple Graft Densities

Chen-Gang Wang,[‡] *Hui Wen Yong,*[‡] and *Atsushi Goto**

Division of Chemistry and Biological Chemistry, School of Physical and Mathematical Sciences, Nanyang Technological University, 21 Nanyang Link, 637371 Singapore

Abstract. This paper reports an effective method to prepare patterned polymer brushes on surfaces with tailored graft densities. High-density (concentrated), moderate-density (semi-dilute), and low-density (dilute) polymer brushes were fabricated in patterned manners, offering defined 3D-patterned structures. This method uses a middle/near-UV (≥ 250 nm) lamp and needs only a short time (≤ 10 min) to fabricate pre-patterns of the initiator, in sharp contrast to the previous high-energy lithography and time-consuming processes. The obtained patterned brush served as a molecular (protein) repellent/adsorptive interface based on a graft-density dependent size-exclusion effect. This method is facile and accessible to wide ranges of tunable density and pattern shape, which are attractive for extensive use.

INTRODUCTION

Polymer brushes on solid surfaces have attracted great attention because they can provide surfaces with desired mechanical, optical, biological, and stimuli-responsive properties.[1–4] The conformation of the brush polymer in a solvent dramatically changes with the graft density (surface occupancy (σ*)) (Figure 1).[5,6] Dilute polymer brushes at low graft densities (σ* ≤ 1~2%, typically) will assume a mushroom conformation. With an increase in the graft density, graft chains start to overlap with each other and are obliged to stretch away from the surface. The stretched brushes are categorized into semi-dilute polymer brushes at moderate graft densities (σ* = 1−10%, typically) and concentrated polymer brushes at high graft densities (σ* ≥ 10%, typically), in which the interaction between polymer chains significantly favours chain extension. Based on the different chain conformations, the graft density significantly influences the physical properties of polymer brushes such as adhesion, friction, and antifouling.[7–9]

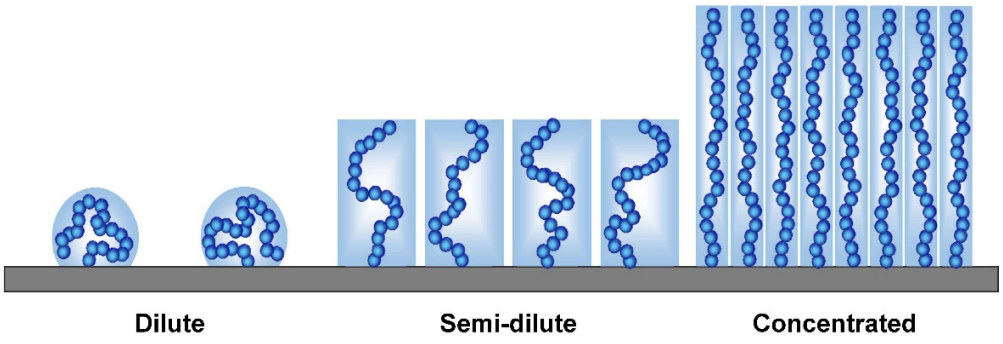

Figure 1. Illustrations of dilute (low-density), semi-dilute (moderate-density), and concentrated (high-density) brushes.

Patterned polymer brushes with different graft densities are of interest because polymer brushes with different physical properties are arranged in two-dimensional (2D) or three

dimensional (3D) patterns. Because of the different properties (*e.g.*, different biocompatibility, molecular recognition, and electron conductivity) arranged on a single surface, the patterned polymer brushes allow applications in, *e.g.*, bio-microarray detection, molecular recognition analytical devices, and microelectronic devices.[10,11] Surface-initiated living radical polymerization has been used to prepare such patterned polymer brushes from pre-patterned initiators.[1,5,6,10−13] Several advanced techniques such as electron-beam lithography,[14,15] interference laser lithography,[16,17] scanning-probe lithography,[18−21] and micro-contact printing[22,23] have successfully been used to prepare the pre-patterned initiators with controlled surface densities. Not only the high-energy beam and laser but also low-energy UV light (≤ 254 nm), plasma, and UV/ozone were exploited to degrade alkyl bromide surface-initiators of atom transfer radical polymerization.[24−29] However, the UV-degradation of the alkyl bromides is time-consuming (≥ 3.5 h), limiting its extensive use.

We have developed an organocatalyzed living radical polymerization, termed reversible complexation mediated polymerization (RCMP), using alkyl iodide (R–I) initiators and organic catalysts.[30−34] In RCMP (Scheme 1), a catalyst (*e.g.*, iodide anion) coordinates the iodide of polymer−I (dormant species) to form a polymer−I---catalyst complex *via* halogen bonding, which is followed by the polymer−I bond cleavage to reversibly generate a propagating radical polymer$^{\bullet}$. Attractive features of RCMP include no use of metals or special sulfur agents and the accessibility to a wide range of functional monomers and polymer architectures including polymer brushes. A unique aspect of RCMP is the use of an R–I initiator that carries a weak carbon-iodide bond. We recently found that R–I initiators immobilized on surface were able to degrade rapidly under middle/near-UV irradiation (250−385 nm).[35] The combination of the UV-degradation and RCMP offered patterned polymer brushes and functional surfaces.

Scheme 1. Reversible Activation in Reversible Complexation Mediated Polymerization.

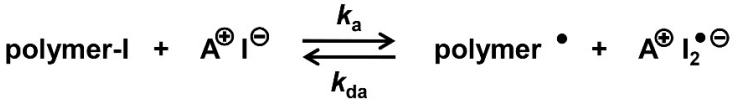

A = tetrabutylammonium, tetraoctylammonium, etc.

In the present work, we further found that the degradation of R–I could be tuned by modulating the UV irradiation intensity. A broad range of the initiator densities were finely attainable through a rapid (≤ 10 min) UV-irradiation (250−385 nm), which is in sharp contrast to the time-consuming (≥ 3.5 h) UV-degradation for alkyl bromides. Using photomasks, we prepared pre-patterned initiators with tailored densities and obtained patterned polymer brushes with multiple (two, three, and four) densities after subsequent polymerization. This synthetic approach gives polymer brushes with tailored graft densities ranging from dilute to semi-dilute and concentrated regions. The facile synthesis and the wide range of the tunable graft density are unique and beneficial features for extensive applications. Moreover, the thickness of polymer brush is proportional to the graft density. The combination of the thickness control (Z-direction) given by the density control and the photomask pattern (XY-direction control) offers 3D-patterned polymer brushes. 3D-patterned polymer structures are emerging structure platforms for biomimetic, microelectronic, sensing, photonic applications.[36−38] Different from the previous methods using advanced equipment, the present method can provide 3D-patterned polymer brushes using more easily accessible equipment. The patterned polymer brushes with different graft densities exhibited regionally different protein repellency based on a size-exclusion effect, indicating its potential applications to molecular or biomolecular recognition interfaces.

EXPERIMENTAL SECTION

Preparation of Alkyl Iodide Initiator-Immobilized Silicon Wafers. A silicon wafer (1 cm × 1 cm) was cleaned with acetone (with sonication for 30 min), chloroform (with sonication for 30 min), and isopropanol (with sonication for 30 min). After drying under nitrogen flow, the wafer was subjected to ozone treatment twice for 15 min each. The wafer was immersed in a mixture of 6-(2-iodo-2-isobutyryloxy)hexyltriethoxysilane (IHE), ethanol, and aqueous ammonia solution (1/89/10 (w/w/w)) at room temperature in a dark condition for one day. The wafer was washed with ethanol, sonicated in ethanol for 30 min, and dried under nitrogen flow to give an IHE-immobilized silicon wafer.

Preparation of Pre-patterned Wafer. A photomask was washed with acetone and dried under nitrogen flow before use. An IHE-immobilized wafer was covered with a photomask and irradiated with a UV lamp (250−385 nm). The wafer was rinsed with acetone and dried under nitrogen flow.

Surface-initiated Polymerization of Poly(methyl methacrylate) (PMMA). A pre-patterned IHE-immobilized silicon wafer was immersed in a mixture of MMA (2.0 g (8000 mM)), 2-iodo-2-methylpropionitrile (CP−I, 1.6 mM), and tetra-*n*-octylammonium iodide (ONI, 40 mM) in a Schlenk flask and heated at 60 °C under argon atmosphere with magnetic stirring for 24 h. (The wafer was inclined to the wall of the Schlenk flask and the stir bar was located underneath the wafer.) After the polymerization, the free polymer obtained was diluted with THF and analyzed with gel permeation chromatography (GPC). The wafer was washed with acetone and dried with nitrogen flow. The thickness of the polymer brush in the dry state was determined with atomic force microscope (AFM). We scratched the brush and measured the height gap between the

scratched and unscratched areas. The thickness of the IHE initiator layer was approximately 2 nm, suggesting that the IHE layer was not a mono-layer but a multi-layer. The brush thickness presented in all tables was corrected (subtracted) by the thickness of the IHE layer.

Calculation of Graft density and Surface occupancy.[5,39]

The graft density (σ) of polymer brushes was calculated using the number average molecular weight (M_n) of free polymer and dry thickness (h) of polymer brushes from eq (1):

$$\sigma = \frac{h\rho N_A}{M_n} \qquad (1)$$

where ρ is the polymer density of the polymer and N_A is Avogadro's number.

The surface occupancy (σ^*) of polymer brushes was calculated using the graft density (σ) and cross-sectional area (a^2) from eq (2):

$$\sigma^* = a^2\sigma \qquad (2)$$

The polymer density of PMMA is 1.19 g/mL (in bulk) and the cross-sectional area of PMMA is 0.554 nm^2.[40] The polymer density and cross-sectional area of poly(2-hydroxyethyl methacrylate) (PHEMA) are 1.15 g/mL (in bulk) and 0.751 nm^2, respectively.[41]

RESULTS AND DISCUSSION

Density Control of Patterned Polymer Brushes. A surface-immobilizing initiator (IHE, Figure 2a) consisting of an alkyl iodide initiating group and a triethoxysilyl anchoring group, was uniformly attached on a silicon wafer. The wafer was irradiated with UV light (250−385 nm, 0.06−0.25 W cm^{-2}) for 5 min using a photomask (Figure S1a), generating a pattern of the initiator (Figure 2b). Subsequently, surface-initiated RCMP was conducted by immersing the

wafer in a mixture of methyl methacrylate (MMA, 8000 mM), a non-immobilized (free) initiator CP−I (Figure 2a, 1.6 mM), and a catalyst ONI (Figure 2a, 40 mM) at 60 °C, yielding a patterned polymer brush (Figure 2b). The free initiator (CP−I) was added because its addition can improve the control over M_n and dispersity ($Đ = M_w/M_n$), where M_n and M_w are the number- and weight-average molecular weights, respectively.[5]

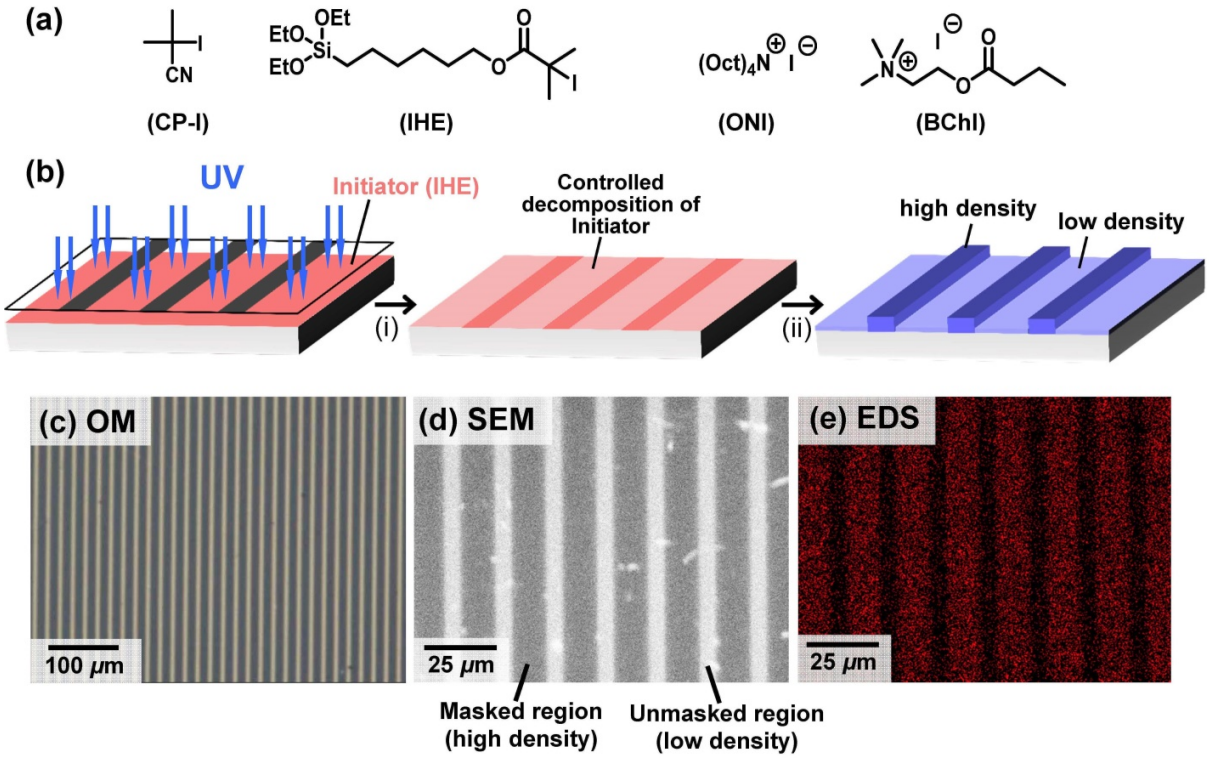

Figure 2. (a) Structures of alkyl iodide initiators and catalysts used in this work. (b) Illustration of the preparation of patterned polymer brushes with controlled graft densities. (i) UV-irradiation for 5 min; (ii) surface-initiated RCMP. (c) OM image, (d) SEM image, (e) EDS carbon distribution map of the patterned polymer brush in Table 1 (entry 6).

A striped photomask (with masked 12 μm and unmasked 6 μm pitches (Figure S1c)) led to a striped pattern of a poly(methyl methacrylate) (PMMA) brush with high-density (masked) and

low-density (unmasked) regions. Figure 2c, 2d, and 2e show the optical microscopy (OM) image, scanning electron microscopy (SEM) image, and energy dispersive x-ray spectroscopy (EDS) carbon distribution map of the obtained polymer brush (Table 1 (Entry 6)). The observed high contrasts clearly demonstrate the generation of a patterned polymer brush with two densities. As a model experiment, we also studied the degradation of IHE in solution (free IHE in solution) with ^{1}H NMR. After 5 min UV-irradiation, 95% of IHE was degraded, confirming the rapid decomposition of IHE (Figure S5).

Table 1 (entries 1−5) and Figure 3 summarize the results using five different UV intensities (0−0.25 W/cm^2). The M_n and $Đ$ of the free polymer obtained from the free initiator are generally in good agreement with those of the surface grafted polymer and were approximately 200000 and 1.2, respectively, in all five studied cases.[5] The dry thickness of the brush was gauged with AFM. In the present work, we used the M_n value of the free polymer for the calculation of the graft density, assuming that the M_n value of the graft polymer is the same as that of the free polymer. In the masked area, IHE was retained, and the brush thickness (60 ± 5 nm) and surface occupancy (σ* = 12−13%) were virtually identical in the five cases (Figure 3). In the unmasked area, IHE was degraded, and the brush thickness linearly decreased from 63 nm to 3 nm (hence σ* decreased from 13% to 1%) with an increase in the UV intensity (Figure 3), demonstrating the tailored synthesis of concentrated (high-density), semi-diluted (moderate-density) and diluted (low-density) brushes by simply changing the UV intensity. The facile and rapid (5 min) operation of the pre-patterning and the wide range of the controllable graft density are notable advantages of this method.

Instead of using the alkyl iodide initiator IHE, we carried out a reference experiment using an alkyl bromide initiator 6-(2-bromo-2-isobutyryloxy)hexyltriethoxysilane (BHE) with the same

chemical structure except the halogen (Br or I) *via* copper-catalyzed atom transfer radical polymerization (ATRP). The BHE-immobilized wafer was covered with a photomask (Figure S1a) and irradiated with UV light (250−385 nm, 0.25 W cm^{-2}) for 5 min and 60 min, followed by surface-initiated ATRP. We obtained polymer brushes on both wafers but with no clear patterns (Figure S6). The thickness in the masked region (31 nm) and unmasked region (31 nm) was the same for the 5 min UV-irradiation (Table S4 (entry 1)). This is in sharp contrast to the result of our IHE initiator for the 5 min UV-irradiation, *i.e.*, the 95% drop of the thickness from the masked region (55 nm) to the unmasked region (3 nm) (Table 1 (entry 5)). Even for a much longer time of 60 min of the UV-irradiation, the brush thickness for the BHE initiator dropped by only 18% (45 nm to 37 nm) (Table S4 (entry 2)). This result means that the irradiation energy (250−385 nm, 0.25 W cm^{-2}) is insufficient for the degradation of bromide initiators in a short time and that the facile and rapid degradation by the UV irradiation is unique to the iodide initiator (IHE).

Table 1. Patterned polymer brushes with controlled graft densities.

Entry[a]	UV energy (W/cm^2)[b]	Conv (%)[c]	M_n[d] ($M_{n,theo}$[e])	$Đ$[d]	Masked region			Unmasked region		
					Thickness (nm)	σ (chains/nm^2)[f]	σ* (%)	Thickness (nm)	σ (chains/nm^2)[f]	σ* (%)
1	0	41	200000 (210000)	1.25	63	0.23	13	63	0.23	13
2	0.06	44	180000 (220000)	1.22	56	0.22	12	41	0.16	9
3	0.12	49	220000 (250000)	1.19	66	0.21	12	34	0.11	6
4	0.18	41	220000 (210000)	1.34	65	0.22	12	22	0.07	4
5	0.25	44	190000 (220000)	1.23	55	0.21	12	3	0.01	1
6	0.25	40	220000 (200000)	1.24	46	0.14	8	9	0.03	2

[a][MMA]$_0$/[CP−I]$_0$/[ONI]$_0$ = 8000/1.6/40 (mM) at 60 °C for 24 h in all cases. The target degree of polymerization at a full (100%) monomer conversion was 5000. Use of striped photomasks with a masked 50 μm and unmasked 25 μm pitch (Figure S1a) for entries 1−5 and a masked 12 μm and unmasked 6 μm pitch (Figure S1c) for entry 6. [b]Degradation of IHE with a UV lamp (250−385 nm wavelength) for 5 min. [c]Monomer conversion determined with ^{1}H NMR. [d]PMMA-calibrated THF-GPC values of the free polymers. [e]Theoretical M_n calculated with [MMA]$_0$, [CP−I]$_0$, and monomer conversion. [f]Calculated from the dry thickness of the brush and the M_n of the free polymer.

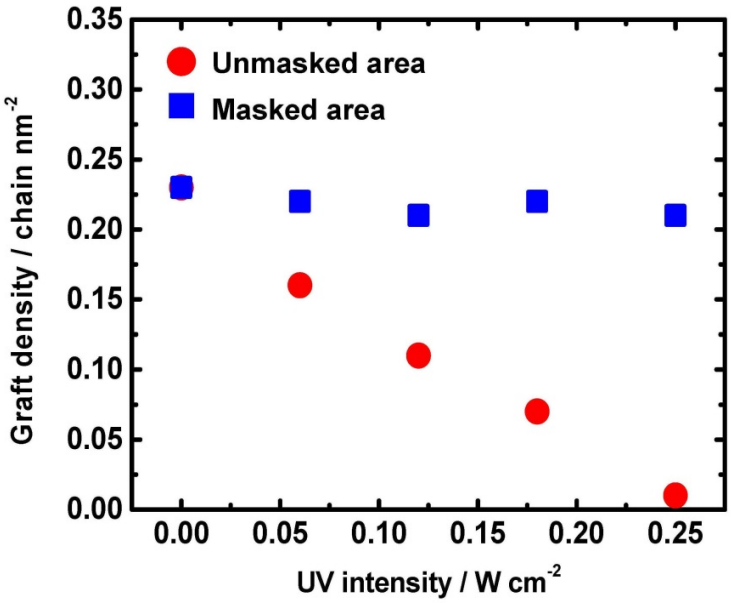

Figure 3. Plot of graft density vs UV intensity (for the degradation of IHE) for patterned polymer brushes in Table 1 (entries 1–5). The symbols are indicated in the figure.

Patterned Polymer Brushes with 3 Different Densities. This method can access not only 2 different densities but also 3 different densities (Table 2 (entries 1−3) and Figure 4). A wafer with uniform IHE was irradiated with UV for 5 min using a striped photomask. The same photomask was then rotated with 90 degrees, and the wafer was irradiated by UV for another 5 min, giving patterned IHE with three different densities (Figure 4a).

Figure 4b shows the OM image of the obtained polymer brush (Table 2 (entry 2)). Three different brush thicknesses were clearly observed as dark (area 1 in Figure 4b, 56 nm thick), medium (area 2, 26 nm thick), and bright (area 3, 10 nm thick) areas. The AFM images (Figure 4c and 4d) display clear boundary steps, confirming the generation of a 3D structure. By varying the UV intensity (0.06, 0.12, and 0.25 W/cm^2), the brush thicknesses were tuned to 63/50/36 nm, 56/26/10 nm, and 65/13/8 nm (Table 2 (entries 1−3) and Figure 4b−4d) and S3). The thicknesses correspond to σ^* (%) = 9/7/5, 10/4/2, and 11/2/1, respectively, again highlighting the accessibility to a tailored combination of concentrated, semi-diluted, and diluted brushes. Using various photomasks (Figure S1), patterned brushes with different shapes and pitches were also obtained (Figure 4e, 4f, and 4g and Table S2), demonstrating the versatility in photomasks and patterns.

Table 2. Patterned PMMA brushes with 3 and 4 different graft densities.

Entry[a]	UV energy (W/cm^2)[b]	Exposure time (min)	Conv (%)[c]	M_n[d] ($M_{n,theo}$[e])	$Đ$[d]	Region[f]	Thickness (nm)	σ (chain/nm^2)[g]	σ* (%)
1	0.06	5.0	44	290000 (220000)	1.31	1	63	0.16	9
						2	50	0.12	7
						3	36	0.09	5
2	0.12	5.0	45	230000 (230000)	1.33	1	56	0.17	10
						2	26	0.08	4
						3	10	0.03	2
3	0.25	5.0	41	240000 (210000)	1.16	1	65	0.19	11
						2	13	0.04	2
						3	8	0.02	1
4	0.06 (1^{st}) 0.12 (2^{nd})	2.5	45	170000 (220000)	1.18	1	63	0.27	15
						2	46	0.19	11
						3	37	0.16	9
						4	29	0.12	7
5	0.06 (1^{st}) 0.12 (2^{nd})	5.0	40	200000 (200000)	1.33	1	50	0.18	10
						2	31	0.11	6
						3	19	0.07	4
						4	8	0.03	2

[a] $[MMA]_0/[CP-I]_0/[ONI]_0$ = 8000/1.6/40 (mM) at 60 °C for 24 h in all cases. The target degree of polymerization at a full (100%) monomer conversion was 5000. [b] Photomask a (Figure S1) was used in all cases. IHE was degraded with a UV lamp (250−385 nm). UV-irradiation was carried out twice. [c] Monomer conversion determined with ^{1}H NMR. [d] PMMA-calibrated THF-GPC values of the free polymers. [e] Theoretical M_n calculated with $[MMA]_0$, $[CP-I]_0$, and monomer conversion. [f] Regions are shown as 1−3 (Entries 1−3) and 1−4 (Entries 4−5) from the thickest brush region (region 1) to the thinnest brush region (region 3 or 4). [g] Calculated from the dry thickness of the brush and the M_n of the free polymer.

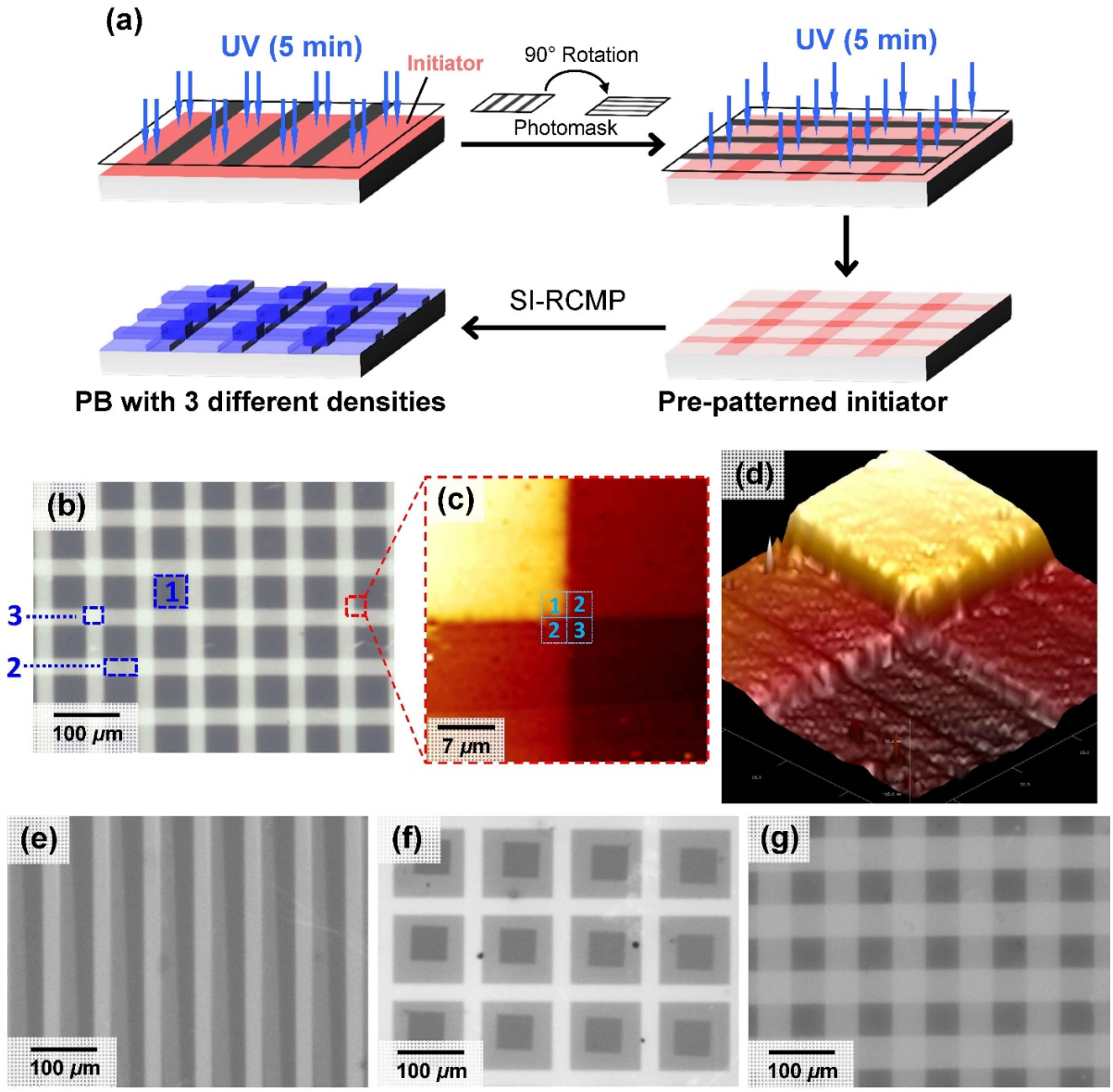

Figure 4. (a) Illustrations of the preparation of patterned polymer brushes with 3 different densities. (b) OM, (c) AFM 2D, and (d) AFM 3D images of the polymer brush obtained in Table 2 (entry 2), respectively. (e,f,g) OM images of the polymer brushes obtained in Table S2 (entries 1, 2, and 3, respectively).

Patterned Polymer Brushes with 4 Different Densities. Furthermore, patterned brushes with 4 different densities were obtained (Figure 5 and Table 2 (entry 4)). Two different UV intensities were used in the first and second irradiation steps. Using a striped photomask, the first irradiation

was exposed at 0.06 W/cm^2 for 2.5 min. After a 90-degree-rotation of the photomask, the second irradiation was applied on the wafer at an increased intensity of 0.12 W/cm^2 for another 2.5 min. The OM, AFM 2D, and AFM 3D images (Figure 5) demonstrated four distinct thicknesses. The UV-irradiation time was prolonged from 2.5 min to 5 min (Figure S4a and Table 2 (entry 5)). The step gap increased from 63/46/37/29 nm (entry 4) to 50/31/19/8 nm (entry 5), which corresponds to σ* (%) = 15/11/9/7 and 10/6/4/2, respectively. Again, concentrated, semi-diluted, and diluted brushes were tailored in a pattern. Thus, this approach enabled a tailored synthesis of 3D patterned brushes with multiple densities from a single initiator (IHE).

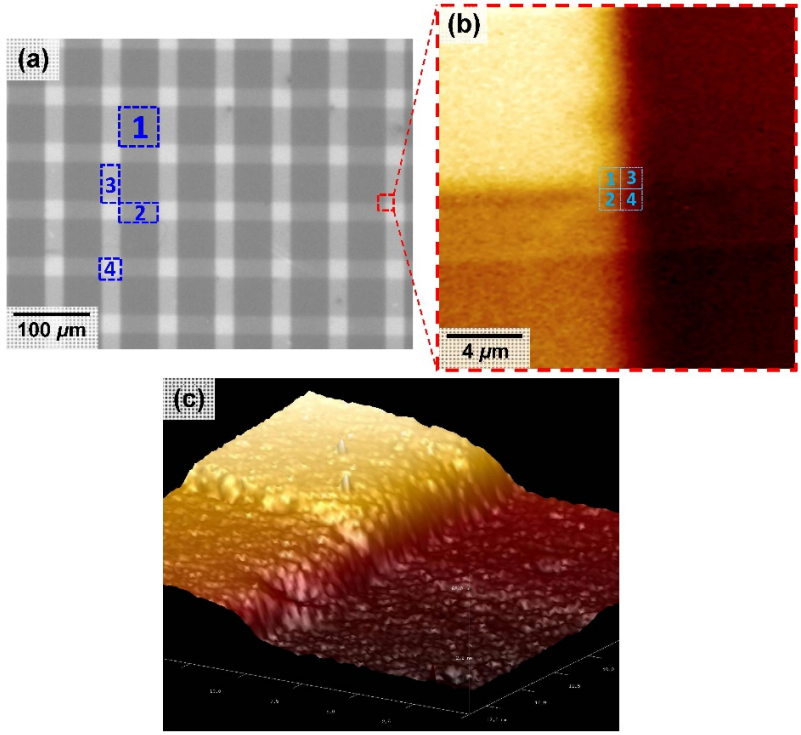

Figure 5. (a) OM, (b) AFM 2D, and (c) AFM 3D images of patterned polymer brush with 4 graft densities (Table 2 (entry 4)), respectively.

Selective Protein Repellency on Patterns. A unique application of the patterned polymer brushes described here is the graft-density-dependent protein adhesion and repellency. Bovine

serum albumin (BSA) protein is highly adhesive to cast coating films and low-density brushes of poly(2-hydroxyethyl methacrylate) (PHEMA).[41] On the other hand, concentrated PHEMA brushes show strong repellency to BSA.[41] We prepared a patterned PHEMA brush with high (σ^* = 8%) and low (σ^* = 2%) densities (Figure 6a and Table S1). The successful application to the PHEMA brush indicates a potentially broad monomer scope of this approach. We used a non-toxic catalyst, butyrylcholine iodide (BChI, Figure 2a), in this synthesis. The use of non-toxic catalyst is attractive for biological applications.[34] The obtained brush was immersed in an aqueous solution of fluorescein isothiocyanate conjugated BSA (FITC-BSA), rinsed with phosphate-buffered saline, and analyzed with fluorescence microscopy (FM).

The FM image (Figure 6b) showed a striped distribution of the adsorbed FITC-BSA. The high-density brush regions were non-fluorescent (without FITC-BSA), while the low-density brush regions were fluorescent (with FITC-BSA). The high-density brush chains highly stretch away from the surface because of the steric hindrance of the neighboring chains (Figure 6c). When a solute molecule is large enough as compared with the distance between graft chains, the size exclusion occurs, preventing the solute molecules from diffusing into the brush layer. In contrast, the low-density brush chains are flexible in their conformation, allowing even large molecules to diffuse into the brush layer (Figure 6c). The studied large molecule FITC-BSA (molecular weight = 67000) was able to diffuse into the low-density regions but not into the high-density regions, because of the size exclusion effect. Thus, the patterned polymer brushes with different graft densities may open up unique molecular and biomolecular recognition interfaces.

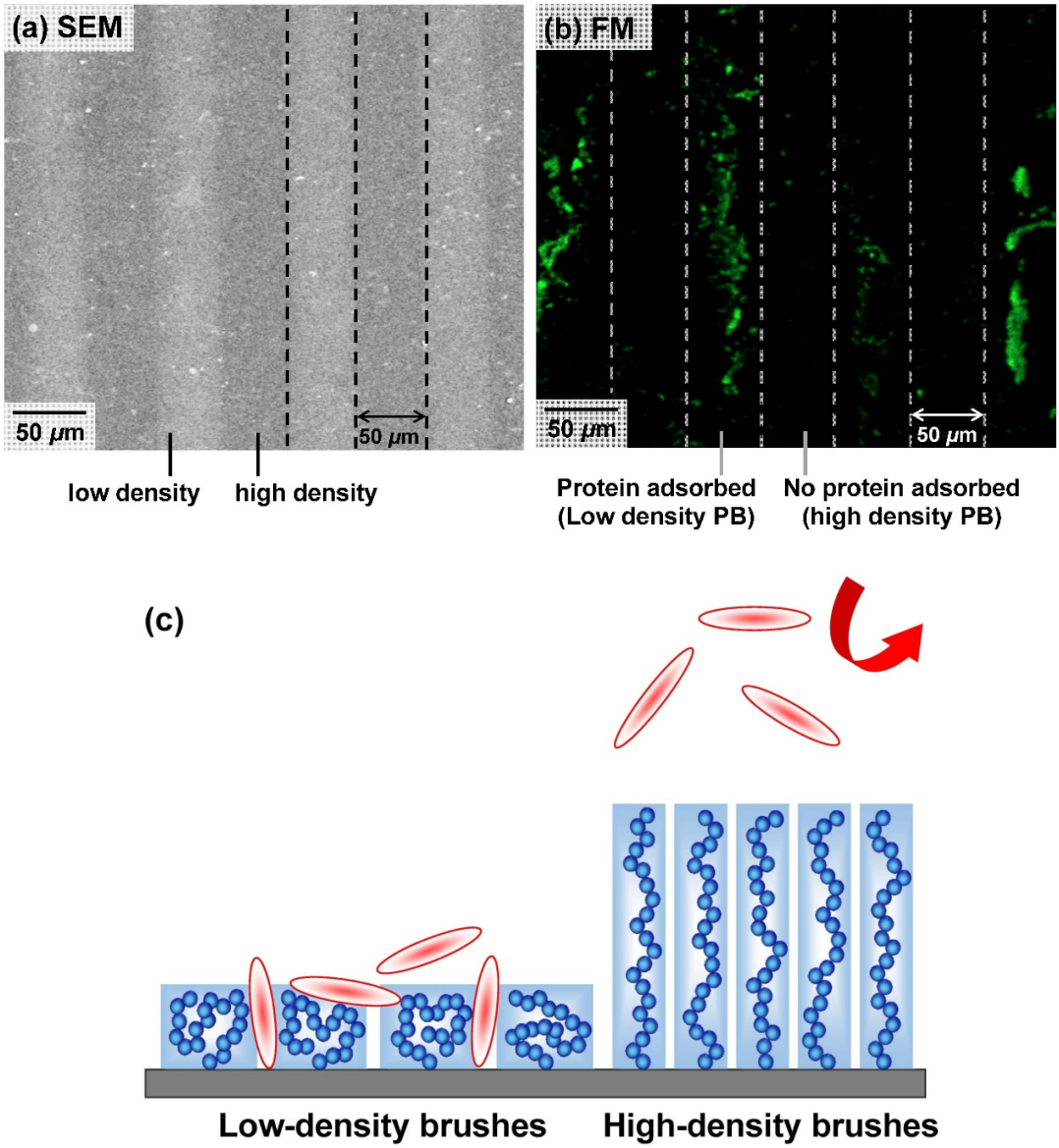

Figure 6. (a) SEM image, and (b) fluorescence microscope (FM) image of patterned PHEMA brushes. The experimental condition is given in Table S1 (entry 1). (c) Schematic illustration of size exclusion effect on the protein repellency and adsorption.

CONCLUSION

In summary, we developed a useful method to construct patterned polymer brushes with tailored graft densities. The R–I initiator was degraded in linear response to the UV-irradiation energy, enabling the control of the initiator density and hence the graft density of the polymer brushes. This finding offered the construction of a range of 3D-patterned polymer brushes with multiple graft densities in various pattern shapes. Notably, a tailored combination of dilute, semi-dilute, and concentrated brushes was attained. Biocompatible PHEMA brushes with different graft densities served as molecular recognition interface, showing a size-exclusion effect on the protein repellency and adsorption. The use of middle/near-UV light, the facile and rapid pre-patterning, the wide range of the tunable density, and the metal-free process are attractive features of this approach.

ASSOCIATED CONTENT

Supporting Information. The Supporting Information is available free of charge on the

ACS Publications website at http://pubs.acs.org.

Materials, measurement, experimental procedures, results of patterned polymer brushes with multiple densities.

AUTHOR INFORMATION

Corresponding Author

*E-mail: agoto@ntu.edu.sg

Author Contributions

‡These authors contributed equally. (C.-G. Wang and H. W. Yong)

ORCID

C.-G Wang: 0000-0001-6986-3961

A. Goto: 0000-0001-7643-3169

Notes

The authors declare no competing financial interest.

ACKNOWLEDGMENT

This work was partly supported by Academic Research Fund (AcRF) Tier 2 from Ministry of Education in Singapore (MOE2017-T2-1-018).

REFERENCES

(1) Chen, W.-L.; Cordero, R.; Tran, H.; Ober, C. K. *50th Anniversary Perspectiv*e: Polymer Brushes: Novel Surfaces for Future Materials. *Macromolecules* **2017**, *50*, 4089−4113.

(2) Keating IV, J. J.; Imbrogno, J.; Belfort, G. Polymer Brushes for Membrane Separations: A Review. *ACS Appl. Mater. Interfaces* **2016**, *8*, 28383−28399.

(3) Yang, W. J.; Neoh, K.-G.; Kang, E.-T.; Teo, S. L.-M.; Rittschof, D. Polymer Brush Coatings for Combating Marine Biofouling. *Prog. Polym. Sci.* **2014**, *39*, 1017−1042.

(4) Chen, T.; Ferris, R.; Zhang, J.; Ducker, R.; Zauscher, S. Stimulus-responsive Polymer Brushes on Surfaces: Transduction Mechanisms and Applications. *Prog. Polym. Sci.* **2010**, *35*, 94−112.

(5) Tsujii, Y.; Ohno, K.; Yamamoto, S.; Goto, A.; Fukuda, T. Structure and Properties of High-Density Polymer Brushes Prepared by Surface-Initiated Living Radical Polymerization. *Adv. Polym. Sci.* **2006**, *197*, 1−45.

(6) Bhat, R. R.; Tomlinson, M. R.; Wu, T.; Genzer, J. Surface-Grafted Polymer Gradients: Formation, Characterization, and Applications. *Adv. Polym. Sci.* **2006**, *198*, 51−124.

(7) Brittain, W. J.; Minko, S. J. A Structural Definition of Polymer Brushes. *Polym. Sci. Part A: Polym. Chem.* **2007**, *45*, 3505−3512.

(8) Krishnamoorthy, M.; Hakobyan, S.; Ramstedt, M.; Gautrot, J. E. Surface-Initiated Polymer Brushes in the Biomedical Field: Applications in Membrane Science, Biosensing, Cell Culture, Regenerative Medicine and Antibacterial Coatings. *Chem. Rev.* **2014**, *114*, 10976−11026.

(9) Galvin, C. J.; Genzer, J. Applications of Surface-grafted Macromolecules Derived from Post-polymerization Modification Reactions. *Prog. Polym. Sci.* **2012**, *37*, 871−906.

(10) Nie, Z.; Kumacheva, E. Patterning Surfaces with Functional Polymers. *Nat. Mater.* **2008**, *7*, 277−290.

(11) Chen, T.; Amin, I.; Jordan, R. Patterned Polymer Brushes. *Chem. Soc. Rev.* **2012**, *41*, 3280−3296.

(12) Zoppe, J. O.; Ataman, N. C.; Mocny, P.; Wang, J.; Moraes, J.; Klok, H.-A. Surface-Initiated Controlled Radical Polymerization: State-of-the-Art, Opportunities, and Challenges in Surface and Interface Engineering with Polymer Brushes. *Chem. Rev.* **2017**, *117*, 1105−1318.

(13) Hui, C. M.; Pietrasik, J.; Schmitt, M.; Mahoney, C.; Choi, J.; Bockstaller, M. R.; Matyjaszewski, K. Surface-Initiated Polymerization as an Enabling Tool for Multifunctional (Nano-)Engineered Hybrid Materials. *Chem. Mater.* **2011**, *26*, 745−762.

(14) Ahn, S. J.; Kaholek, M.; Lee, W. K.; LaMattina, B.; LaBean, T. H.; Zauscher, S. Surface□ Initiated Polymerization on Nanopatterns Fabricated by Electron□Beam Lithography. *Adv. Mater.* **2004**, *16*, 2141−2145.

(15) Ballav, N.; Schilp, S.; Zharnikov, M. Electron-Beam Chemical Lithography with Aliphatic Self-Assembled Monolayers. *Angew. Chem. Int. Ed.* **2008**, *47*, 1421−1424.

(16) Schuh, C.; Santer, S.; Prucker, O.; Rühe, J. Polymer Brushes with Nanometer-Scale Gradients. *Adv. Mater.* **2009**, *21*, 4706−4710.

(17) Adams, J.; Tizazu, G.; Janusz, S.; Brueck, S. R. J.; Lopez, G. P.; Leggett, G. J. Large-Area Nanopatterning of Self-Assembled Monolayers of Alkanethiolates by Interferometric Lithography. *Langmuir* **2010**, *26*, 13600−13606.

(18) Kaholek, M.; Lee, W.-K.; LaMattina, B.; Caster, K. C.; Zauscher, S. Fabrication of Stimulus-Responsive Nanopatterned Polymer Brushes by Scanning-Probe Lithography. *Nano Lett.* **2004**, *4*, 373−376.

(19) Zhou, X.; Wang, X.; Shen, Y.; Xie, Z.; Zheng, Z. Fabrication of Arbitrary Three-Dimensional Polymer Structures by Rational Control of the Spacing between Nanobrushes. *Angew. Chem. Int. Ed.* **2011**, *50*, 6506−6510.

(20) Xie, Z.; Zhou, X.; Tao, X.; Zheng, Z. Polymer Nanostructures Made by Scanning Probe Lithography: Recent Progress in Material Applications. *Macromol. Rapid Commun.* **2012**, *33*, 359−373.

(21) Bog, U.; de los Santos Pereira, A.; Mueller, S. L.; Havenridge, S.; Parrillo, V.; Bruns, M.; Holmes, A. E.; Rodriguez-Emmenegger, C.; Fuchs, H.; Hirtz, M. Clickable Antifouling Polymer Brushes for Polymer Pen Lithography. *ACS Appl. Mater. Interfaces* **2017**, *9*, 12109−12117.

(22) Zhou, F.; Zheng, Z.; Yu, B.; Liu, W.; Huck, W. T. S. Multicomponent Polymer Brushes. *J. Am. Chem. Soc.* **2006**, *128*, 16253−16258.

(23) Chen, T.; Jordan, R.; Zauscher, R. Dynamic Microcontact Printing for Patterning Polymer-Brush Microstructures. *Small*, **2011**, *7*, 2148−2152.

(24) Iwata, P.; Suk-In, V. P.; Hoven, A.; Takahara, A.; Akiyoshi, K.; Iwasaki, Y. Control of Nanobiointerfaces Generated from Well-Defined Biomimetic Polymer Brushes for Protein and Cell Manipulations. *Biomacromolecules* **2004**, *5*, 2308−2314.

(25) Tugulu, S.; Harms, M.; Fricke, M.; Volkmer, D.; Klok, H.□A. Polymer Brushes as Ionotropic Matrices for the Directed Fabrication of Microstructured Calcite Thin Films. *Angew. Chem. Int. Ed.* **2006**, *44*, 7458−7461.

(26) Li, L.; Nakaji-Hirabayashi, T.; Kitano, H.; Ohno, K.; Kishioka, T.; Usui, Y. Gradation of Proteins and Cells Attached to the Surface of Bio-inert Zwitterionic Polymer Brush. *Colloids Surf. B: Biointerfaces* **2016**, *144*, 180−187.

(27) Li, L.; Nakaji-Hirabayashi, T.; Kitano, H.; Ohno, K.; Saruwatari, Y.; Matsuoka, K. A Novel Approach for UV-patterning with Binary Polymer Brushes. *Colloids Surf. B: Biointerfaces* **2018**, *161*, 42−50.

(28) Saboohi, S.; Coad, B. R.; Michelmore, A.; Short, R. D.; Griesser, H. J. Hyperthermal Intact Molecular Ions Play Key Role in Retention of ATRP Surface Initiation Capability of Plasma Polymer Films from Ethyl *α*-Bromoisobutyrate. *ACS Appl. Mater. Interfaces* **2016**, *8*, 16493−16502.

(29) Sheridan, R. J.; Orski, S. V.; Muramoto, S.; Stafford, C. M.; Beers, K. L. Ultraviolet/Ozone as a Tool To Control Grafting Density in Surface-Initiated Controlled-Radical Polymerizations via Ablation of Bromine. *Langmuir* **2016**, *32*, 8071−8076.

(30) Goto, A.; Suzuki, T.; Ohfuji, H.; Tanishima, M.; Fukuda, T.; Tsujii, Y.; Kaji, H. Reversible Complexation Mediated Living Radical Polymerization (RCMP) Using Organic Catalysts. *Macromolecules* **2011**, *44*, 8709−8715.

(31) Goto, A.; Ohtsuki, A.; Ohfuji, H.; Tanishima, M.; Kaji, H. Reversible Generation of a Carbon-Centered Radical from Alkyl Iodide Using Organic Salts and Their Application as Organic Catalysts in Living Radical Polymerization. *J. Am. Chem. Soc.* **2013**, *135*, 11131−11139.

(32) Ohtsuki, A.; Lei, L.; Tanishima, M.; Goto, A.; Kaji, H. Photocontrolled Organocatalyzed Living Radical Polymerization Feasible over a Wide Range of Wavelengths. *J. Am. Chem. Soc.* **2015**, *137*, 5610−5617.

(33) Wang, C.-G.; Goto, A. Solvent-Selective Reactions of Alkyl Iodide with Sodium Azide for Radical Generation and Azide Substitution and Their Application to One-Pot Synthesis of Chain-End-Functionalized Polymers. *J. Am. Chem. Soc.* **2017**, *139*, 10551−10560.

(34) Wang, C.-G.; Hanindita, F.; Goto, A. Biocompatible Choline Iodide Catalysts for Green Living Radical Polymerization of Functional Polymers. *ACS Macro Lett.* **2018**, *7*, 263−268.

(35) Wang, C.-G.; Chen, C.; Sakakibara, K.; Tsujii, Y.; Goto, A. Facile Fabrication of Concentrated Polymer Brushes with Complex Patterning by Photocontrolled Organocatalyzed Living Radical Polymerization. *Angew. Chem. Int. Ed.* **2018**, *57*, 13504−13508.

(36) Zhou, X.; Liu, X.; Xie, Z.; Zheng, Z. 3D-patterned Polymer Brush Surfaces. *Nanoscale* **2011**, *3*, 4929−4939.

(37) Sun, T.; Qing, G. Biomimetic Smart Interface Materials for Biological Applications. *Adv. Mater.* **2011**, *23*, H57−H77.

(38) Bae, W.-G.; Kim, H. N.; Kim, D.; Park, S.-H.; Jeong, H. E.; Suh, K.-Y. 25th Anniversary Article: Scalable Multiscale Patterned Structures Inspired by Nature: the Role of Hierarchy. *Adv. Mater.* **2014**, *26*, 675−700.

(39) Malham, I. B.; Bureau, L. End-Grafted Low-Molecular-Weight PNIPAM Does Not Collapse above the LCST. *Langmuir* **2010**, *26*, 4762−4768.

(40) Yamamoto, S.; Ejaz, M.; Tsujii, Y.; Fukuda, T. Surface Interaction Forces of Well-Defined, High-Density Polymer Brushes Studied by Atomic Force Microscopy. 2. Effect of Graft Density. *Macromolecules* **2000**, *33*, 5608−5612.

(41) Yoshikawa, C.; Goto, A.; Tsujii, Y.; Fukuda, T.; Kimura, T.; Yamamoto, K.; Kishida, A. Protein Repellency of Well-Defined, Concentrated Poly(2-hydroxyethyl methacrylate) Brushes by the Size-Exclusion Effect. *Macromolecules* **2006**, *39*, 2284−2290.

for Table of Contents use only